Model diagnosis of nighttime minimum temperature warming during summer due to irrigation in the California Central Valley

by

Hideki Kanamaru and Masao Kanamitsu

Scripps Institution of Oceanography

University of California, San Diego

Submitted to

Journal of Hydrometeorology

August 17, 2007

Revised December 14, 2007

Corresponding Author: Dr. Hideki Kanamaru

University of California, San Diego

9500 Gilman Drive, MC-0224, La Jolla, CA, 92093-0224, USA.

Phone: +1-858-822-3847. Fax: +1-858-534-8561. email: hkanamaru@ucsd.edu

Abstract

This study examines the mechanisms of nighttime minimum temperature warming in the California Central Valley during summer due to irrigation. The Scripps Experimental Climate Prediction Center (ECPC) Regional Spectral Model (RSM) was used to simulate climate under two land surface characteristics: potential natural vegetation and modern land use that includes irrigation and urbanization. In irrigated cropland, soil moisture was prescribed in three different ways: 1) field capacity, 2) half of field capacity, and 3) no addition of water. In the most realistic case of half field capacity, July daily minimum temperature in the California Central Valley increased by 3.5 ºC, in agreement with station observation trends over the past century in the same area. It was found that ground heat flux efficiently keeps the surface warm during nighttime due to increased thermal conductivity of wet soil.

1. Introduction

The importance of land-cover change has received increasing attention in recent years. Feddema et al. (2005) suggest that significantly different regional climates in 2100 can be projected by adding the effects of changes in land cover to atmospheric forcing scenarios. The Western United States has undergone significant land use change in the past 150 years. Irrigation has been used on over 35000 km^2 in California alone (USDA 2004). We can expect significant climate change over the Western United States, due solely to the change in the land use.

Observational studies have shown that irrigation is one of the largest factors to influence near surface climate. Barnston and Schickedanz (1984) found that irrigation cools summer daily maximum temperatures by 1-2 ºC in the Texas Panhandle. Daily minimum temperatures showed no trend. Mahmood et al. (2004) and Mahmood et al. (2006) found a decreasing trend in daily maximum temperature under irrigated land use in Nebraska. Both dry and irrigated land showed an increase in minimum temperature. In the same irrigated area, Adegoke et al. (2003) found a decreasing trend in maximum temperature and very little trend in minimum temperature.

Over the Western United States, Christy et al. (2006; hereafter referred to as C06) presented an analysis of temperature observations in the California Central Valley (where most irrigated cropland is located) and the adjacent highlands during the twentieth century. They developed a method to generate composite time series of weather station data and compared the valley results (*Valley*; 18 stations) with those of the adjacent highlands (*Sierra*; 23 stations) to examine the response in near-surface air temperature to the changes in the valley surface conditions. *Valley* daily minimum temperature time series show a significant positive trend in all seasons, especially in JJA and SON (about 3 ºC per century). *Sierra* JJA daily minimum temperature shows a significant cooling trend (about 2 ºC per century) but other *Sierra* trends are small. The difference between the *Valley* and the *Sierra* time series shows a significant positive trend for the *Valley* daily minimum temperature, peaking in JJA, at over 0.5 ºC per decade, i.e., a relative warming of 5 ºC in *Valley* JJA daily minimum temperature compared to the *Sierra* over the last century. They hypothesized that the relative positive trends in the Central Valley are related to the modified surface conditions due to the growth of irrigated agriculture in the region.

There have been recent studies in which climate models were used to simulate the effects of irrigation on climate. On the global scale, Boucher et al. (2004) found a mean surface air temperature cooling of up to 0.8ºC over irrigated areas. Lobell et al. (2006) showed local surface cooling of up to 8ºC and global land surface cooling of 1.3ºC due to irrigation. The cooling was much stronger for daily maximum than minimum temperatures, decreasing the diurnal temperature range. A large number of other studies used regional climate models to study the impacts of irrigation. Adegoke et al. (2003) simulated decreasing near surface temperature in irrigated land in Nebraska. De Ridder and Gallee (1998) found a decreased diurnal temperature range due mainly to warmer minimum temperatures in irrigated areas.

Thus, there seems to be a consensus that irrigation leads to a decreased daily maximum temperature. However, observations and model studies produce mixed signals for the impacts of irrigation on daily minimum temperature.

Recently, climate research groups in California have conducted a model intercomparison study of the climate response to land use change in the Western United States (Kueppers et al. 2007; hereafter referred to as K07). Four regional climate models, the International Center for Theoretical Physics (ICTP) Regional Climate Model RegCM3 (Pal et al. 2007), which includes the Biosphere-Atmosphere Transfer Scheme (BATS1E) (Dickinson et al., 1993), the NCAR/Penn State (PSU) Mesoscale Model version 5.v3.6 (MM5) coupled with the NCAR Community Land Model version 3 (CLM3) (Jin and Miller 2007), the Davis Regional Climate Model (DRCM) coupled with a modified version of the Noah land surface model (Chen and Dudhia, 2001), and the Scripps Experimental Climate Prediction Center (ECPC) Regional Spectral Model (RSM) coupled with the Oregon State University Land Scheme (OSU, Mahrt and Pan, 1984; Pan and Mahrt, 1987), were run with two different land cover datasets – potential natural vegetation and modern land use (including urbanization and irrigation). All the models showed large decreases in August mean and maximum 2-meter air temperatures where irrigation replaced natural vegetation. However, in the irrigated area, only RSM produced a large *increase* in August minimum 2-meter air temperature. Other models produced either a small change or a significant decrease.

The major purpose of this paper is to analyze in detail the increase in daily minimum temperature in the California Central Valley due to change in land use in the RSM simulation. This increase agrees with the observational study by C06, and we hope to find physically possible processes which may occur over irrigated land during nighttime that raise the minimum temperature. We will first examine the relation between the assumptions made to the soil moisture over irrigated areas and the magnitude of changes in the annual cycle of temperature guided by the land surface water budgets. We will then examine the surface energy budget to diagnose the mechanisms of the change in daytime and nighttime surface skin temperatures and near surface air temperatures in summer months before and after irrigation, our major focus being the warming of nighttime minimum temperature due to irrigation.

2. Experiments and model

The modern land cover that includes urbanization and irrigation was derived from the Global Land Cover Characteristics (GLCC) database. The potential natural land cover was created from the GLCC data by replacing anthropogenic types with their nearest-neighbor natural vegetation types. The land cover dataset preparation is discussed in detail in K07.

The model was run at 25 km resolution over the area shown in Figure 1 with potential natural vegetation (NAT) and modern land cover that includes irrigated agriculture and urban areas (MOD). The National Centers for Environmental Prediction (NCEP) and Department of Energy (DOE) Reanalysis II (Kanamitsu et al. 2002) was used as lateral boundary forcing. CO_2 concentrations were held constant at 348ppm for the experiment period. Other radiatively active materials, such as aerosols and other greenhouse gases, were the same in NAT and MOD cases. The model archives outputs every hour and the plotted temperature is the instantaneous value at that hour. Daily maximum and minimum near surface temperatures are separately archived throughout the model run.

The version of the RSM (Juang and Kanamitsu, 1994) used for this study was originally developed at NCEP, and subsequently updated at ECPC in the Scripps

Institution of Oceanography (SIO) (Kanamitsu et al., 2005). The RSM applies sine and cosine series to the deviation of the full forecast field from the global base field (perturbations), and is capable of performing accurate and efficient evaluation of prediction equations (Juang and Kanamitsu, 1994). A "scale selective bias correction scheme" (Kanamaru and Kanamitsu, 2006) was used to reduce error relative to the reanalysis in the large-scale (>1000km) fields within the regional domain. The land surface model is OSU. It includes 12 United States Geological Survey (USGS) vegetation types and two more types for irrigated cropland and urban land that have been added for this study. There are 16 soil types from the State Soil Geographic Database (STATSGO; Miller and White 1998). Soil properties were specified by the analysis of Cosby et al. (1984) and were held constant between the NAT and MOD cases. OSU has two soil layers. The top layer is 10 cm thick and the bottom layer is 190 cm thick.

Although the two soil-layer specification of the OSU land surface model is simple compared to state-of-the-art models including better representations of bottom layer drainage and thin upper layer (Ek et al. 2003; Maxwell and Miller, 2005), OSU has demonstrated reasonable diurnal and seasonal cycles of soil moisture (Mahrt and Pan 1984; Pan and Mahrt 1987). Pitman et al. (2004) looked at the complexity level of land surface models and its impact on differences in the results of phase 2 of the Atmospheric Model Intercomparison Project. They found that large variations in the complexity of surface energy balance schemes did not result in systematic differences in the simulated mean, minimum, and maximum temperature variance at the global scale and in the zonal averages. DeHaan et al. (2007), in their comparison of the OSU land surface model and the newer four-layer Noah model, found that OSU is not necessarily inferior to Noah despite its simpler parameterizations. Noah produced a large warm bias of temperature climatology in the northern latitudes in JJA and SON, while OSU was closer to reanalysis. In the tropics the magnitudes of the biases are similar between the two. The precipitation climatology bias was also similar in magnitude between the two. For the temporal anomaly correlations with observations, Noah was more skillful in three seasons for near surface temperature and was more skillful in one season for precipitation. There was no significant difference in precipitation skill in the other three seasons. The results of these land surface model comparisons do not discourage the use of OSU in the current study. It should be noted that the current study benefited from the simple soil specifications of OSU that facilitated simple parameterization of irrigated water and interpretation of the energy flux and temperature changes. We plan to use the RSM coupled with the four-layer Noah land surface model in future studies.

NAT vegetation type in irrigated areas was replaced by a unique cropland vegetation type (ID #13) in the MOD case. Soil type spatial distribution is independent of vegetation cover and was not changed for the experiments, but soil thermal properties vary by soil moisture content. In order to simulate the extra water available for the irrigated area, RSM assumed that the soil was saturated in irrigated areas all the time in the intercomparison paper K07. However, the saturation produced an excessive amount of ground water drainage and may not be a good representation of irrigated soil.

In the K07 validation of the MOD results using the Climatic Research Unit's observational data, all four models captured the broad patterns in January 2m daily mean air temperature, with cool biases in DRCM and MM5-CLM3 in parts of Nevada and a warm bias in RSM in Central California. All four models also captured regional variations in August 2m daily mean air temperature except in the California Central Valley, where the three models that supplemented soil moisture (RSM, RegCM3 and DRCM) to irrigated cropland showed a cool bias. RSM and RegCM3 also underestimated the daily maximum temperature in parts of the Central Valley. There was less bias in MM5-CLM3, which did not supplement soil moisture. Soil moisture was probably prescribed too high in the irrigation parameterization of the first three models.

For this study, three experiments with more realistic specifications of soil moisture in irrigated areas were performed for two years from October 1995 (following the experiments in K07) with hourly outputs. In order to avoid spin-up, only the result from the second year (October 1996 to September 1997) is presented. In the experiments discussed in this study, irrigation water parameterizations were turned on throughout the simulation years. Although the real agricultural field is not irrigated every day of the year, the conclusion of the study did not change when the soil moisture parameterization was applied only for the summer.

Other models in K07 varied in the manner by which soil moisture was altered to mimic irrigation in the irrigated cropland vegetation type. RegCM3-BATS1E set soil moisture to field capacity at all time steps and replaced natural soil types with loam. DRCM-Noah set the artificial soil moisture source rate to 4.8225×10^{-8} ms^{-1} when the top soil layer temperature is greater than 12°C, and zero when less than 12°C. MM5-CLM3 did not manipulate soil moisture. In these two models soil types are parameterized separately from vegetation types.

In our first experiment soil moisture in the top soil layer was set at field capacity at every time step (MOD-fld). In the second experiment the top soil layer soil moisture was supplemented to half of field capacity at every time step when falling below a half field capacity level (MOD-halfld). The last experiment did not manipulate soil moisture in order to see the effect of vegetation change only (MOD-nowater).

The changes of temperature and surface energy budget between the MOD and NAT cases partly depend on the soil type and NAT vegetation type. There are 3703 land grid cells in the simulation domain, and 133 of them (4 %) are irrigated cells in the MOD case. 35 % (47 cells) of the irrigated agricultural area (vegetation type 13) in the MOD case was converted from vegetation type 2 (tall/medium grassland and shrubland) in the NAT case. 34 % (45 cells) of the irrigated area was originally vegetation type 9 (medium grassland and woodland). The three vegetation types and their properties are listed in Table 1. Soil types 4 (silt loam, 38 %, 50 cells) and 3 (sandy loam, 23 %, 30 cells) are prevalent in the irrigated agricultural area in this study and their properties are listed in Table 2. The dominant combination of soil type and NAT vegetation type in the California Central Valley is soil type 3 and vegetation type 9 and the area is shown in Figure 1. The area is referred to as CCV (22 cells) and the study hereafter discusses the results of sensitivity experiments over the CCV area.

3. Results and discussion

3.1 Annual cycle

Figure 2 shows the sizes of three MOD cases' daily minimum near surface (2 m above ground) temperature changes, with respect to the NAT case, over the CCV area. The annual cycle is plotted for October 1996 to September 1997. Daily minimum near surface temperature is warmer in all MOD cases than in the NAT case throughout the year except for the MOD-nowater and MOD-halfld cases in December 1996. The wetter the soil the warmer the minimum temperature is. Warming is larger in October, March, and July. Also plotted in Figure 2 are two measures for the significance of minimum temperature change in the CCV area. One is a standard deviation of minimum temperature from a 6 member ensemble run with different initial conditions (dating back one each day from the start time of the simulation). The standard deviation does not exceed 0.03 ^{o}C in any month. The other measure is a standard deviation of year-to-year variability of minimum temperature from 57-year 10 km downscaling of NCEP-NCAR reanalysis over California (CaRD10), which does not include land use change (Kanamitsu and Kanamaru 2007). Summer minimum temperature changes in the MOD-halfld and MOD-fld cases are statistically significant, exceeding twice the standard deviation.

Using station observations, C06 found an approximate 3ºC decrease of maximum near surface temperature and a 3ºC increase of minimum temperature over the past century in summer months in the California Central Valley. All three MOD cases in the CCV area produce the same direction of changes in maximum and minimum near surface temperatures as the station observations (not shown). The MOD-fld case may be exaggerating the effects of irrigation because maximum near surface temperature decreased by 8.9ºC in July and minimum temperature warmed by about 4.5ºC. Because of the irrigation water parameterization, soil moisture in both soil layers remains constant throughout the year (Figure 3.a and 3.b) and much of the excess water is drained as ground water runoff (Figure 3.c) without being used in evapotranspiration (Figure 3.d). The MOD-fld case supplies more water than crops need and apparently too much water was added to the soil.

The California Department of Water Resources publishes crop water use and evapotranspiration data (http://www.landwateruse.water.ca.gov/). The evapotranspiration rate from a crop surface with specific characteristics, not short of water, is called the reference crop evapotranspiration (FAO, 1998). It is used for computing crop water requirements. The crop evapotranspiration in the Central Valley is about 800 mm for the average of all crop types in the growing season. Depending on the crop type and its growing dates crop evapotranspiration varies, but July mean evapotranspiration is estimated to be about 6.6 mm day^{-1} in the Central Valley (Irrigation Training and Research Center 2003). The MOD-fld and MOD-halfld cases in the CCV area produce realistic amounts of July evapotranspiration (6.2 and 3.0 mm day^{-1}, respectively), which is a considerable increase from the NAT case's 0.7 mm day^{-1} (Figure 3.d). A part of the increased evapotranspiration can be explained by vegetation property change. The MOD-nowater case does not artificially add water to soil to mimic irrigated water, yet it produces larger latent heat flux than the NAT case. Irrigated cropland vegetation has much lower stomatal resistance than the NAT vegetation (Table 1) so transpiration is enhanced in the MOD cases. From winter to summer soil moisture levels become lower as water is lost through evapotranspiration. The MOD-nowater case uses the top soil layer moisture more slowly than the NAT case (Figure 3.a) but the second soil layer moisture falls to lower moisture content in the summer than the NAT case (Figure 3.b). Water supplied from the second soil layer is able to meet the additional water demand by enhanced transpiration. MOD-halfld follows the same annual cycle of second layer soil moisture as MOD-nowater.

The MOD-halfld case in the CCV area produced a 3.8 ºC decrease of July maximum temperature and a 3.5 ºC increase of July minimum temperature. This is the most realistic scenario considering the size of the temperature trend of station observations. Also, there is no waste of water due to ground water runoff in the summer months (Figure 3.c). Although a large ground water runoff was produced in January when the CCV area received precipitation, the NAT and MOD-nowater cases also produced groundwater runoff in the same month.

3.2 Diurnal cycle

From here we focus on temperature changes in July 1997 to examine the mechanism of summertime minimum temperature warming. The daily minimum temperature discussed above is the air temperature at 2 m above the ground. The diurnal cycle of near surface temperature in July 1997 in the CCV area is shown in Figure 4.a. Nighttime temperature is warmer for wetter soil and reaches its minimum at around 1300 UTC (5:00 a.m. local time). Daytime temperature is cooler for wetter soil and reaches its maximum at around 00 UTC (4:00 p.m. local time). The diurnal variation of land surface skin temperature (Figure 4.b) is larger than that of near surface temperature. The near surface temperature response to wet soil is also true for skin temperature. That is, wetter soil produces warmer nighttime temperatures and cooler daytime temperatures.

We will examine the surface energy budget that determines surface skin temperature in the model, in the most realistic case of MOD-halfld. The 2 m temperature is affected by horizontal and vertical advection, and vertical diffusion, in addition to surface skin temperature. We will discuss the difference between the skin temperature and the 2 m temperature in section 4.

All energy fluxes that affect surface temperature are archived by the model. These energy fluxes are latent heat flux (LHT), sensible heat flux (SHT), ground heat flux (GHT), reflected shortwave radiation (USW), incoming shortwave radiation (DSW), incoming longwave radiation (DLW), and upward longwave radiation (ULW) at the surface. Instantaneously at every time step the energy balance for an infinitely thin model surface layer can be written as:

$$DSW + DLW = USW + ULW + LHT + SHT + GHT \quad (1)$$

The left hand side is radiative heating of the surface, and the processes that remove energy from the surface are on the right hand side. Surface skin temperature is determined in the model by solving the energy balance equation for ULW and the Stefan-Boltzmann constant.

Figure 5.a shows the diurnal cycle of the changes in surface energy fluxes from the NAT to MOD-halfld case in the CCV area. All fluxes are plotted such that the direction pointing to the surface layer is positive and the values are averages of the preceding hour. Latent and sensible heat fluxes are positive downward from the atmosphere to the surface and the sum of the two is plotted because two fluxes change in an offsetting manner. Ground heat flux is positive upward from the top soil layer to the surface. For shortwave radiation, downward flux minus upward flux is plotted. The residual of all these fluxes equals upward longwave radiation, which determines the

surface skin temperature from the Stefan-Boltzmann law (the model assumes unit emissivity).

The CCV irrigated area has a larger albedo than NAT vegetation type 9, so the shortwave radiation received by the surface has decreased. There were no significant changes in cloudiness or incoming shortwave radiation. In any case, shortwave radiation does not affect the energy balance at the time of daily minimum temperature.

Evapotranspiration is enhanced during daytime and upward sensible heat flux decreases in exchange (Figure 5.b) in the CCV area. Part of the increase in evapotranspiration is explained by the lower stomatal resistance of the irrigation land cover specification because the MOD-nowater case also produces increased evapotranspiration. Extra water added to the soil by irrigated water parameterization accounts for the rest of the increased evapotranspiration. During nighttime the changes in these two fluxes are small and they do not affect the daily minimum temperature energy balance.

Increased downward longwave radiation during nighttime indicates near surface air warming, and decreased downward longwave radiation during daytime is a result of cooler air in the CCV area. However, this flux change is relatively smaller than others.

The largest flux change at the time of daily minimum temperature (1300 UTC) is found in ground heat flux which increases by 20 W/m^2 from the NAT to the MOD-halfld case in the CCV area. Ground heat flux is a function of soil thermal conductivity and the temperature difference between skin surface and the top soil layer (Figure 5.c). During nighttime soil temperature is higher than skin temperature so the ground heat flux is upward (Figure 5.d). Skin temperature increases while soil temperature decreases, and the temperature gradient decreases from the NAT to the MOD-halfld case. In spite of the decreased temperature gradient, ground heat flux increases in MOD-halfld. This is because thermal conductivity increases rapidly as soil becomes wetter, which outweighs the decreased temperature gradient. The NAT thermal conductivity of 0.2 $Wm^{-1}K^{-1}$ increases to about 1.1 $Wm^{-1}K^{-1}$ in MOD-halfld. During daytime wetter soil effectively transfers energy from the surface to the soil, decreasing the rate of surface skin warming. During nighttime, ground heat flux keeps the surface warm by providing energy to the surface. The ground heat stored during the daytime conducts from the soil to the surface during nighttime as indicated by the change of the sign of ground heat flux during the night (Fig. 5d). The heat exchange between the surface skin and the soil more than doubles from the NAT to the MOD-halfld case (Fig. 5.d). Enhanced ground heat flux reduces the diurnal range of the surface skin temperature. In response to the surface energy gain due to ground heat flux changes, upward longwave flux increases during nighttime. This is a direct indication of increased skin temperature.

3.3 Diurnal temperature cycles of MOD-cases

Most of the temperature changes from NAT to MOD-halfld are attributed to extra water in the soil rather than the vegetation change to cropland because the MOD-nowater case is closer to NAT than to the other two MOD cases (Figures 2 and 4). We reexamine the effect of irrigated water by comparing three MOD cases.

A plot of the diurnal cycle of temperatures (near surface, surface skin, top soil layer, and bottom soil layer; Figure 6.a) in the MOD-nowater case shows that the near surface temperature warms slowly and lags behind the surface skin temperature by 2-3 hours during the daytime, but these two temperature diurnal cycles are in sync and cool at the same rate during nighttime. The top soil layer temperature has a much smaller diurnal variation than those two temperatures. The bottom soil layer temperature does not change diurnally due to its large heat capacity. In the MOD-halfld case (Figure 6.b) near surface temperature follows surface skin temperature more closely, closing the temperature difference between the two during daytime. The top soil temperature has a much larger diurnal variation than in the MOD-nowater case and the diurnal cycle looks similar to those of the near surface and skin temperatures. In the extreme case of MOD-fld (Figure 6.c) the three temperature diurnal cycles are indistinguishable.

In short, the drier top layer soil of the MOD-nowater case only responds to the diurnal change of surface skin temperature slowly because of low soil thermal conductivity. Wetter soil in the MOD-halfld increases conductivity. Top layer soil exchanges heat with the surface skin more efficiently throughout the day, and follows the diurnal cycle of surface skin temperature more closely, resulting in cooler nighttime soil and warmer daytime soil than MOD-nowater. In the MOD-fld case, heat exchanges between soil and surface skin occur almost instantaneously, and the temperature diurnal cycles of the two are almost the same.

3.4 Soil thermal conductivity

The discussion so far has focused on the CCV area with NAT vegetation type 9 and soil type 3. The conclusion did not change for other irrigated areas in the Western United States with different combinations of soil and vegetation types, but the size of daily minimum temperature warming varied. The experiments suggested that the warming magnitude could depend largely on the soil thermal conductivity profile with respect to soil moisture.

In a neighborhood of the CCV area with NAT vegetation type 9 and soil type 4, July 1997 daily minimum temperature increased by 2.0°C in the MOD-halfld case, as opposed to 3.5°C for the CCV. This is likely a consequence of the fact that silt loam's (soil type 4) thermal conductivity does not increase as steeply as that of sandy loam (soil type 3) for a higher soil moisture fraction (Figure 7).

The RSM coupled with OSU uses a function for computing the thermal conductivity by Al Nakshabandi and Kohnke (1965) and McCumber and Pielke (1981). However, Peters-Lidard et al. (1998) suggested that this function may overestimate (underestimate) conductivity for wet (dry) soil, in comparison to the data collected in the First International Satellite Land Surface Climatology Project (ISLSCP) Field Experiment (FIFE), and proposed a new function after Johansen (1975).

The new function was incorporated in the Noah land surface scheme and a newer version of the RSM is coupled with the Noah that has soil properties defined for 9 soil types. Two soil types prevalent in the Central Valley are silty clay loam and light clay. Thermal conductivities for these soils as a function of soil moisture are presented in Figure 7. Conductivities of the Noah soils are higher for drier soil but the rate of increase with respect to soil moisture is much smaller for wetter soil than the OSU soils. We are planning to carry out an experiment with the RSM-Noah as a next step.

If the RSM-Noah is used for the same experiment as the current study, it should produce a summertime daily minimum temperature warming of smaller magnitude than the RSM-OSU because the thermal conductivity increase from the NAT to the MOD case is likely to be smaller. This speculation is consistent with the behavior of one of the models in the model intercomparison paper K07. The DRCM coupled with Noah produced a 0.1°C warming of August daily minimum temperature, as opposed to 2.0°C for RSM-OSU in K07. Although the direction of the daily minimum temperature change from natural vegetation to irrigated cropland is very likely to be positive, the size of the increase could vary widely depending on the soil thermal conductivity formulation.

As for other models in K07, MM5-CLM3 did not modify soil moisture for irrigated cropland and it did not produce a minimum temperature warming. RegCM3-BATS1E's soil types are tied to land cover type. Thus, the conversion of natural vegetation to irrigated cropland accompanied a conversion of soil type and the nighttime ground heat flux change cannot be explained easily. The change of soil type seemed to have had a greater impact on the nighttime surface energy balance than the soil wetness change in RegCM3-BATS1E. Although the model added water to soil up to field capacity at all time steps, the August daily minimum temperature decreased in irrigated land.

3.5 Near surface temperature

The surface energy budget examined in the previous section explains the change in the daily minimum surface skin temperature, which is not always the same as the near surface temperature. We will make qualitative arguments on the relationship between surface skin temperature and near surface air temperature. In the model, near surface temperature is calculated as a weighted mean of the surface skin temperature and the temperature at the lowest model level, which is assumed to be the top of the surface layer, using static stability, vertical wind sheer and roughness length based on surface layer theory. However, the greatest factor that determines the near surface temperature in irrigated land is not the weight but the temperature at the lowest model level. The temperature at this level is determined from the thermodynamic equation, including horizontal and vertical advection, and adiabatic cooling, but the major contributor is the vertical diffusion process which is formulated following the non-local diffusion by Hong and Pan (1996). At the lowest model level, the temperature tendency is determined by the difference between the incoming sensible heat flux from the surface skin and the outgoing upward heat flux computed from the vertical diffusion formulation. This upward heat flux is dependent on the static stability and wind sheer. At the time of daily minimum temperature (5:00 a.m.) near surface air is warmer than the surface skin. Therefore, the surface layer tends to be shallow, and we expect the near surface (2-meter) and skin temperatures to be close together (Figure 6.a-c). Thus warming of the surface skin temperature from the NAT to the MOD case implies warming of the near surface temperature. During daytime, when no water is supplemented (NAT and MOD-nowater cases), the surface skin is much warmer than near surface air, thus the surface layer is deep. We expect stronger and deeper mixing in the planetary boundary layer, which results in cooling at the lower PBL levels, with the strongest cooling at the lowest model level. Thus, 2-meter temperature, which is a weighted mean of surface skin and lowest model level temperature, becomes lower. Accordingly, the difference between 2-meter air and the surface skin becomes large (Figure 6.a). In the MOD-halfld and MOD-fld cases, the surface skin temperatures are much colder than those of the NAT and MOD-nowater cases and the surface layer is shallower, leading to less temperature difference. Thus, the surface skin temperatures and the lowest model level temperatures are similar

(Figure 6.b-c). The diurnal variation of near surface air temperature becomes closer to that of the ground skin temperature as the soil becomes wetter.

3.6 Non-local impacts

The daily minimum temperature increase in summer was found not only in those grid cells where natural vegetation was replaced by irrigated cropland but also in adjacent cells, albeit to a smaller extent. The propagation of temperature change was confined to immediate neighboring areas up to two grid cells from irrigated land.

The MOD cases produced slight increases in surface pressure over irrigated areas, which led to small changes on surface winds. Wetter soil in the MOD-halfld case produced larger daytime cooling than nighttime warming. This results in a daily mean temperature cooling of 0.7 ^{o}C in the Central Valley (July 1997). The surface pressure increased up to 0.3 hPa. As a result, the low-level westerlies into the Central Valley weakened and winds out of the valley got stronger, up to 0.8 ms^{-1}. These are the only atmospheric dynamics changes from the NAT to MOD cases. The effects were limited to the boundary layer and did not extend to pressure height and wind above 850 hPa.

4. Summary and Conclusions

Impacts of irrigated cropland on climate in the California Central Valley were investigated using the Regional Spectral Model. The model was run with natural vegetation cover and with modern land cover that includes irrigation and urbanization. Soil moisture was supplemented in irrigated cropland in three different ways: 1) field capacity, 2) half of field capacity, and 3) no addition of water.

Daily minimum near surface temperature becomes warmer when the soil moisture content is larger in our simulation. An analysis of the MOD-halfld case showed that the dominant energy term that determines the daily minimum surface skin temperature is ground heat flux, which warms the surface due to increased soil thermal conductivity. The daily minimum temperature warming signal is statistically significant in the summer, and it is likely that the conclusions from the two-year simulation of this study would not change for a longer-term simulation.

C06 hypothesized several ways in which land use change to irrigated cropland may lead to an increase in daily minimum temperature. Their most plausible theory is that the lower albedo of the vegetation (compared to an almost bare surface) and increased heat capacity of wetter soil enhance nighttime sensible heat flux. In the current study the albedo for the MOD cases was slightly larger than NAT in the CCV area but the daily minimum temperature still resulted in warming, so the change in albedo does not seem to be the largest factor. However, the potential contribution of lower albedo to nighttime warming, through nighttime release of larger daytime solar energy storage, cannot be discounted in the real world. We examined the energy balance at the surface and qualitatively discussed the translation of surface temperature changes into near surface changes. Nighttime sensible heat flux in NAT is negative because near surface air is warmer than the surface. In MOD-halfld the sensible heat flux become less negative, implying less loss of energy during nighttime from the perspective of the near surface air energy balance. The current study proposes a physical mechanism at the surface, which is in line with C06's hypothesis, but highlights the importance of thermal conductivity and ground heat flux.

Finally, it should be noted that the mechanisms presented in this paper are those found in a particular regional climate model and do not necessarily explain the real mechanisms of observed historical temperature changes in irrigated land. In order to validate our result it would be necessary to obtain detailed observations of soil temperature at different soil levels, and of heat conductivity and its dependency on water content, which are not readily available. There are also a number of other factors that could affect the diurnal range of near surface temperature, such as greenhouse gases and aerosols, which are not included in this study. However, the current study suggests that the extra soil moisture provided by irrigation practices has caused warming in the nighttime near surface temperatures in the California Central Valley.

Acknowledgements

This work was funded by the California Energy Commission Public Interest Energy Research (PIER) program, which supports the California Climate Change Center. The authors thank G. Franco for his assistance in performing the research. Thanks to S. Hong for his help on model physics. The assistance of Diane Boomer in refining the writing is appreciated. Comments by three anonymous reviewers are appreciated. This paper originated from a model intercomparison project. The authors thank all the collaborators in the project: L.M. Kueppers, M.A. Snyder, L.C. Sloan (UCSC), D. Cayan, M. Tyree (SIO), J. Jin, N.L. Miller (LBNL), H. Du, H., and B. Weare (UCD).

References

Adegoke, J. O., R. A. Pielke, J. Eastman, R. Mahmood, and K. G. Hubbard, 2003: Impact of irrigation on midsummer surface fluxes and temperature under dry synoptic conditions: a regional atmospheric model study of the U.S. High Plains. *Mon. Wea. Rev.*, **131**, 556-564.

Al Nakshabandi, G., and H. Kohnke, 1965: Thermal conductivity and diffusivity of soils as related to moisture tension and other physical properties. *Agric. Meteorol.*, **2**, 271-279.

Alpert P. and M. Mandel, 1986: Wind variability – an indicator for a mesoclimate change in Israel. *J. Climate Appl. Meteor.*, **25**, 1568-1576.

Barnston, A. G. and P. T. Schickedanz, 1984: The effect of irrigation on warm season precipitation in the Southern Great Plains. *J. Appl. Meteor.*, **23**, 865-888.

Boucher, O., G. Myhre, and A. Myhre, 2004: Direct human influence of irrigation on atmospheric water vapour and climate. *Climate Dyn.,* **22**, 597-603.

Chen, F. and J. Dudhia, 2001: Coupling and advanced land surface-hydrology model with the Penn State-NCAR MM5 modeling system. Part I: Modeling implementation and sensitivity. *Mon. Wea. Rev.*, **129**, 569-585.

Christy, J.R., W.B. Norris, K. Redmond, and K.P. Gallo, 2006: Methodology and Results of Calculating Central California Surface Temperature Trends: Evidence of Human-Induced Climate Change? J. Climate, 19, 548–563.

Cosby, B. J., G. M. Hornberger, R. B. Clapp, and T. R. Ginn, 1984: A statistical exploration of the relationships of soil moisture characteristics to the physical properties of soils. *Water Resour. Res.*, **20**, 682-690.

De Ridder, K., and H. Gallee, 1998: Land surface-induced regional climate change in Southern Israel. *J. Appl. Meteor.*, **37**, 1470-1484.

DeHaan, L. L, M. Kanamitsu, C. -H. Lu, and J. Roads, 2007: A Comparison of the Noah and OSU Land Surface Models in the ECPC Seasonal Forecast model. *J. Hydrometeor*., **8**, 1031-1048.

Dickinson, R. E., A. Henderson-Sellers, and P. J. Kennedy, 1993: Biosphere-Atmosphere Transfer Scheme (BATS) Version 1e as Coupled to the NCAR Community Climate Model. NCAR TN-387+STR, NCAR, Boulder, CO.

Ek, M. B., K. E. Mitchell, Y. Lin, E. Rogers, P. Grunmann, V. Koren, G. Gayno, and J. D. Tarpley, 2003: Implementation of Noah land surface model advances in the National Centers for Environmental Prediction operational mesoscale Eta model. *J. Geophys. Res*., **108(D22)**, 8851, doi:10.1029/2002JD003296.

Feddema, J. J., K. W. Oleson, G. B. Bonan, L. O. Mearns, L. E. Buja, G. A. Meehl, and W. M. Washington, 2005: The importance of land-cover change in simulating future climates. *Science*, **310**, 1674-1678.

Food and Agriculture Organization of the United Nations, 1998: Crop evapotranspiration – Guidelines for computing crop water requirements – FAO irrigation and drainage paper 56. FAO, Rome, Italy. (available from http://www.fao.org/docrep/X0490E/X0490E00.htm)

Hong, S. -Y. and H. -L. Pan, 1996: Nonlocal boundary layer vertical diffusion in a medium-range forecast model. *Mon. Wea. Rev.*, **124**, 2322-2339.

Irrigation Training and Research Center. 2003: California Crop and Soil Evapotranspiration. ITRC, California Polytechnic State University, San Luis

Obispo, California, USA. (available from http://www.itrc.org/reports/californiacrop/californiacrop.htm)

Jin, J. and N. L. Miller, 2007: Coupling of an advanced land surface model with MM5 to improve regional snow simulations. Submitted to *J. Geophys. Res*.

Johansen, O., 1975: Thermal conductivity of soils, Ph.D. thesis, University of Trondheim, 236 pp. [Available from Universitets-biblioteket I Trondheim, Høgskoleringe 1, 7034 Trondheim, Norway.]

Juang, H. -M. and M. Kanamitsu, 1994: The NMC Nested Regional Spectral Model. *Mon. Wea. Rev*., **122**, 3-26.

Kalthoff, N., M. Fiebig-Wittmaack, C. Meißner, M. Kohler, M. Uriarte, I. Bischoff-Gauß, and E. Gonzales, 2006: The energy balance, evapo-transpiration and nocturnal dew deposition of an arid valley in the Andes. *Journal of Arid Environments*, **65**, 420-443.

Kanamaru. H., and M. Kanamitsu, 2007: Scale Selective Bias Correction in Downscaling of Global Analysis Using a Regional Model. *Mon. Wea. Rev*., **135 (2)**, 334–350.

Kanamitsu, M., W. Ebisuzaki, J. Woolen, J. Potter, and M. Fiorino, 2002: NCEP/DOE AMIP-II Reanalysis (R-2). *Bull. Amer. Meteor. Soc*., **83**, 1631-1643.

Kanamitsu, M., H. Kanamaru, Y. Cui, and H. Juang, 2005: Parallel implementation of the regional spectral atmospheric model. CEC-500-2005-014, California Energy Commission, Sacramento, California.

Kueppers, L. M. et al., 2007: Seasonal temperature responses to land-use change in the western United States. *Global and Planetary Change* (2007), doi:10.1016/j.gloplacha.2007.03.005

Lobell, D. B., G. Bala, and P. B. Duffy, 2006: Biogeophysical impacts of cropland management changes on climate. *Geophys. Res. Lett.*, **33**, L06708, doi:10.1029/2005GL025492.

Mahmood, R., K. G. Hubbard, and C. Carlson, 2004: Modification of growing-season surface temperature records in the Northern Great Plains due to land-use transformation: verification of modeling results and implication for global climate change. *Int. J. Climatol.*, **24**, 311-327.

Mahmood, R., S. A. Foster, T. Keeling, K. G. Hubbard, C. Carlson, and R. Leeper, 2006: Impacts of irrigation on 20th century temperature in the northern Great Plains. *Global and Planetary Change.*, **54**, 1-18.

Mahrt, L. and H. Pan, 1984: A two-layer model of soil hydrology. *Bound.-Layer Meteor.*, **29**, 1-20.

Malek, E., G. McCurdy, and B. Giles, 1999: Dew contribution to the annual water balances in semi-arid desert valleys. *Journal of Arid Environments*, **42**, 71-80.

Maxwell, R. M. and N. L. Miller, 2005: Development of a coupled land surface and groundwater model. *J. Hydrometeor.*, **6**, 233-247.

McCumber, M. C., and R. A. Pielke, 1981: Simulation of the effects of surface fluxes of heat and moisture in a mesoscale numerical model soil layer. *J. Geophys. Res.*, **86**, 9929-9938.

Miller, D. A., and R. A. White, 1998: A conterminous United States multilayer soil characteristics dataset for regional climate and hydrology modeling. *Earth Interactions*, **2**, 1-26. [Available online at EarthInteractions.org.].

Pal, J. S. et al., 2007: The ICTP RegCM3 and RegCNET: Regional Climate Modeling for the Developing World. *Bull. Amer. Meteor. Soc*., in press.

Pan, H. L. and L. Mahrt, 1987: Interaction between soil hydrology and boundary-layer development. *Bound.-Layer Meteor*., **38(1-2)**, 185-202.

Pitman, A. J., B. J. McAvaney, N. Bagnoud, and B. Cheminat, 2004: Are inter-model differences in AMIP-II near surface air temperature means and extremes explained by land surface energy balance complexity?, *Geophys. Res. Lett*., **31**, L05205, doi:10.1029/2003GL019233.

Segal, M., Z. Pan, R. W. Turner, and E. S. Takle, 1998: On the potential impact of irrigated areas in North America on summer rainfall caused by large-scale systems. *J. Appl. Meteor*., **37**, 325-331.

USDA, 2004: 2002 Census of Agriculture. USDA National Agricultural Statistics Service.

Figure captions

Figure 1 Irrigated cropland of the California Central Valley with NAT vegetation type 9 and soil type 3 (CCV area). Other irrigated areas in the Western United States are also highlighted.

Figure 2 Daily minimum temperature changes (ºC) for the CCV area from the NAT case to three MOD cases (October 1996 to September 1997). 2*STDV-1: twice the standard deviation of daily minimum temperature for the CCV area from ensemble runs. 2*STDV-2: twice the standard deviation of interannual variability of daily minimum temperature for the CCV area from CaRD10.

Figure 3 Annual cycle of land surface water budget for the CCV area (October 1996 to September 1997). a) top soil layer moisture (m^3/m^3), b) bottom soil layer moisture (m^3/m^3), c) ground water runoff (mm day^{-1}), and d) latent heat flux (mm day^{-1}).

Figure 4 Diurnal cycle of near surface temperature and surface skin temperature for July 1997 in the CCV area.

Figure 5 Diurnal cycle of land surface energy fluxes and temperature for July 1997 in the CCV area. Time in UTC. a) Surface energy flux changes from the NAT case to MOD-halfld case. lht+sht: sum of latent and sensible heat fluxes (positive downward), dlw: downward longwave radiation, gflx: ground heat flux (positive upward), sw: downward shortwave minus upward shortwave, res: residual in the surface energy balance from all other fluxes; equals upward longwave flux. b) Changes in latent and sensible heat fluxes and their sum (positive downward) for the NAT case to MOD-halfld case. c) Surface skin temperature minus top soil layer temperature for the NAT and three MOD cases. d) Ground heat flux (positive upward). NAT and three MOD cases.

Figure 6 Diurnal cycle of near surface, surface skin, top soil layer, and bottom soil layer temperatures for July 1997. a) MOD-nowater, b) MOD-halfld, and c) MOD-fld.

Figure 7 Soil thermal conductivity as a function of volumetric soil moisture for two soil types in RSM-OSU and two soil types in RSM-Noah.

TABLE 1. List of vegetation types

Vegetation type	tall/medium grassland and shrubland	medium grassland and woodland	Irrigated agriculture
Vegetation ID	2	9	13
Roughness length (m)	0.0672	0.4744	0.06
Minimum stomatal resistance (s/m)	300	400	40
Albedo VIS	0.13	0.08	0.10
Albedo NIR	0.32	0.28	0.30

TABLE 2. List of soil types

Soil type	Sandy loam	Silt loam
Soil ID	3	4
Porosity	0.434	0.476
Field capacity	0.312	0.360
Wilting point	0.047	0.084

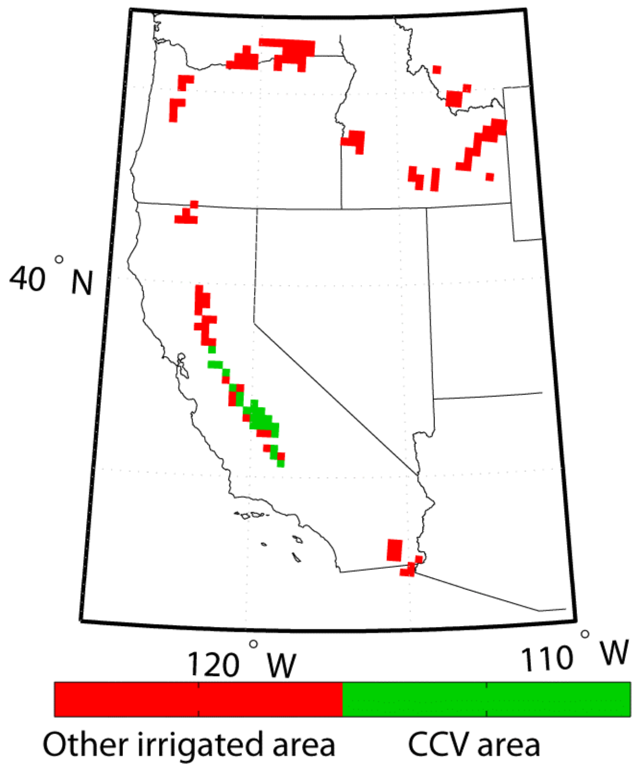

Figure 1 Irrigated cropland of the California Central Valley with NAT vegetation type 9 and soil type 3 (CCV area). Other irrigated areas in the Western United States are also highlighted.

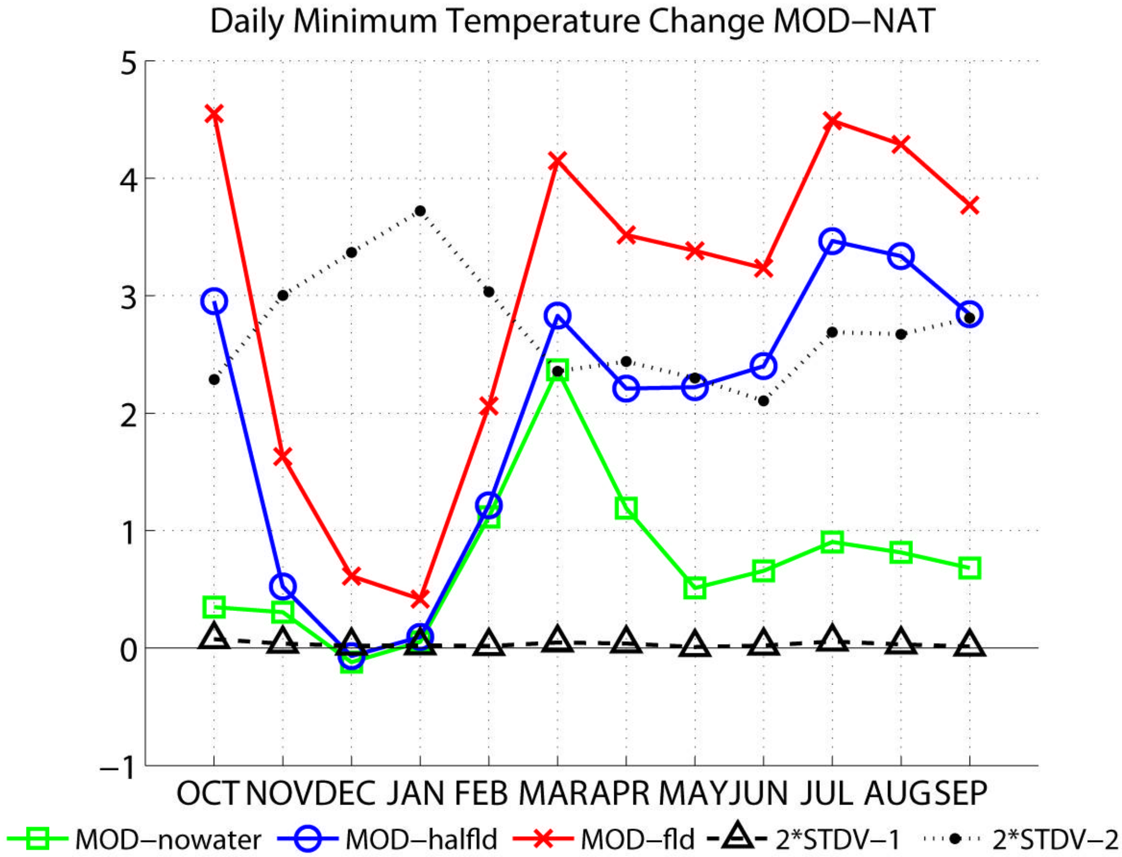

Figure 2 The size of three MOD cases' daily minimum near surface (2 m above ground) temperature change (ºC), with respect to the NAT case, over the CCV area. The annual cycle is plotted for October 1996 to September 1997. 2*STDV-1: twice the standard deviation of daily minimum temperature for the CCV area from ensemble runs. 2*STDV-2: twice the standard deviation of interannual variability of daily minimum temperature for the CCV area from CaRD10.

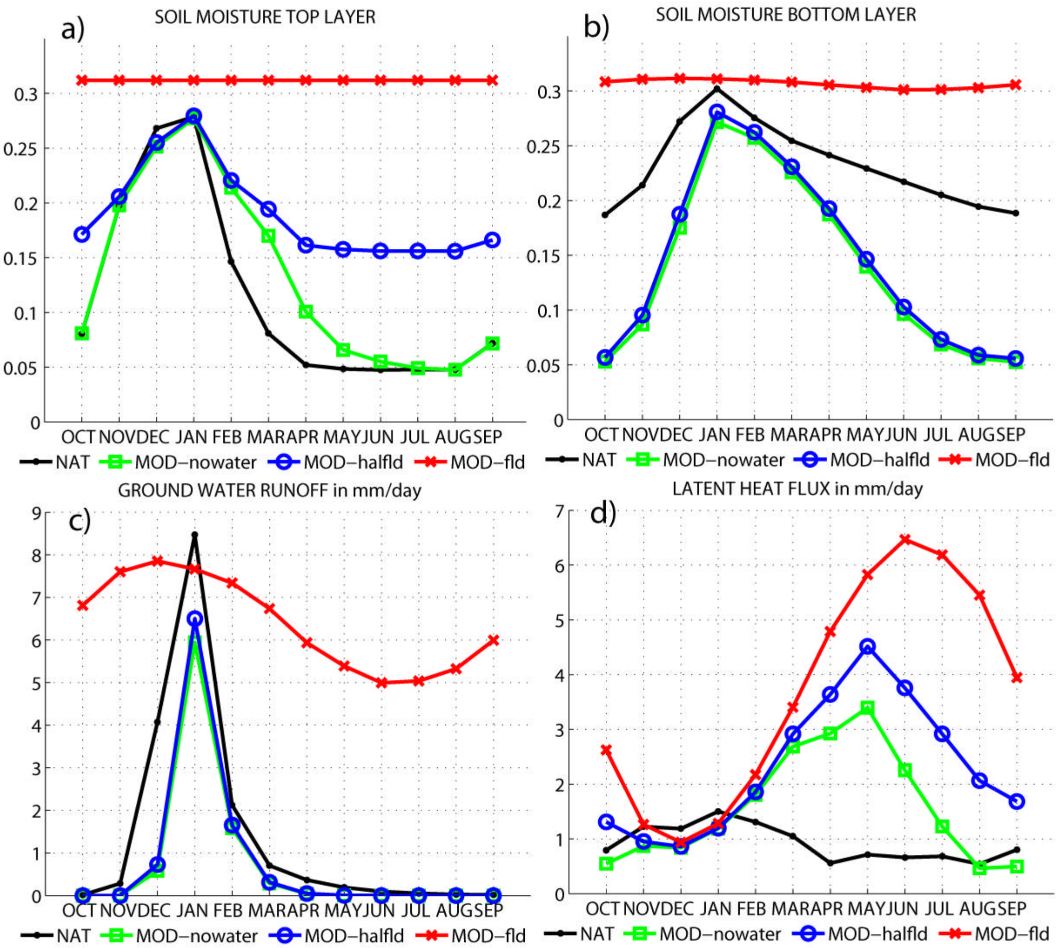

Figure 3 Annual cycle of land surface water budget for the CCV area (October 1996 to September 1997). a) top soil layer moisture (m^3/m^3), b) bottom soil layer moisture (m^3/m^3), c) ground water runoff (mm day^{-1}), and d) latent heat flux (mm day^{-1}).

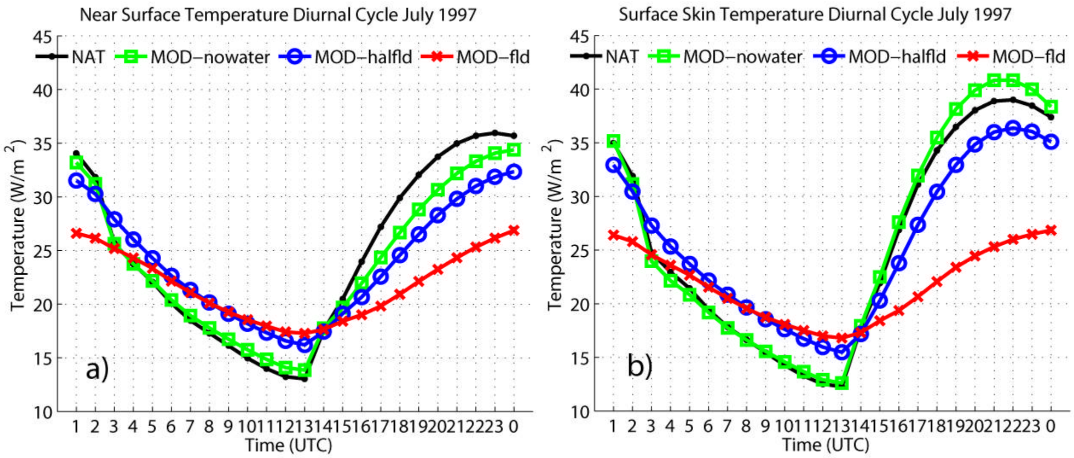

Figure 4 Diurnal cycle of near surface temperature and surface skin temperature for July 1997 in the CCV area.

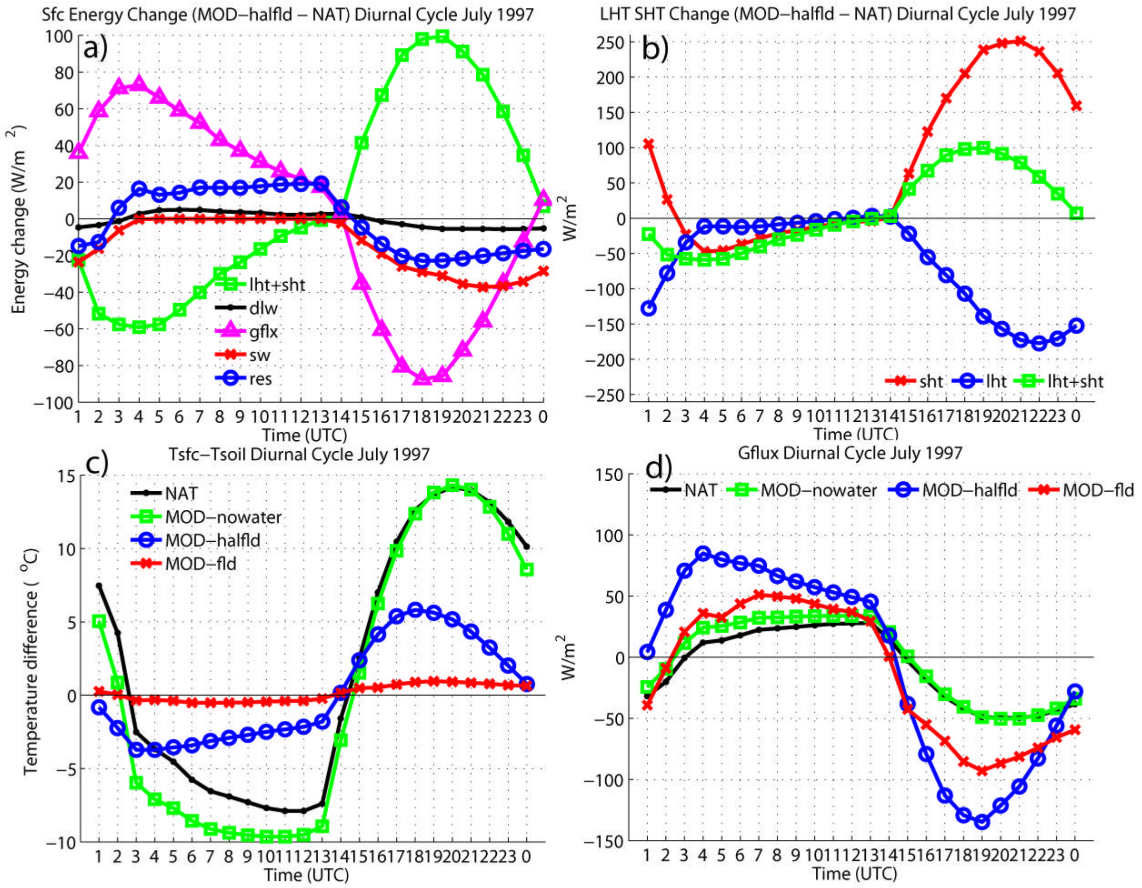

Figure 5 Diurnal cycle of land surface energy fluxes and temperature for July 1997 in the CCV area. Time in UTC. a) Surface energy flux changes from the NAT case to MOD-halfld case. lht+sht: sum of latent and sensible heat fluxes (positive downward), dlw: downward longwave radiation, gflx: ground heat flux (positive upward), sw: downward shortwave minus upward shortwave, res: residual in the surface energy balance from all other fluxes; equals upward longwave flux. b) Changes in latent and sensible heat fluxes and their sum (positive downward) for the NAT case to MOD-halfld case. c) Surface skin temperature minus top soil layer temperature for the NAT and three MOD cases. d) Ground heat flux (positive upward). NAT and three MOD cases.

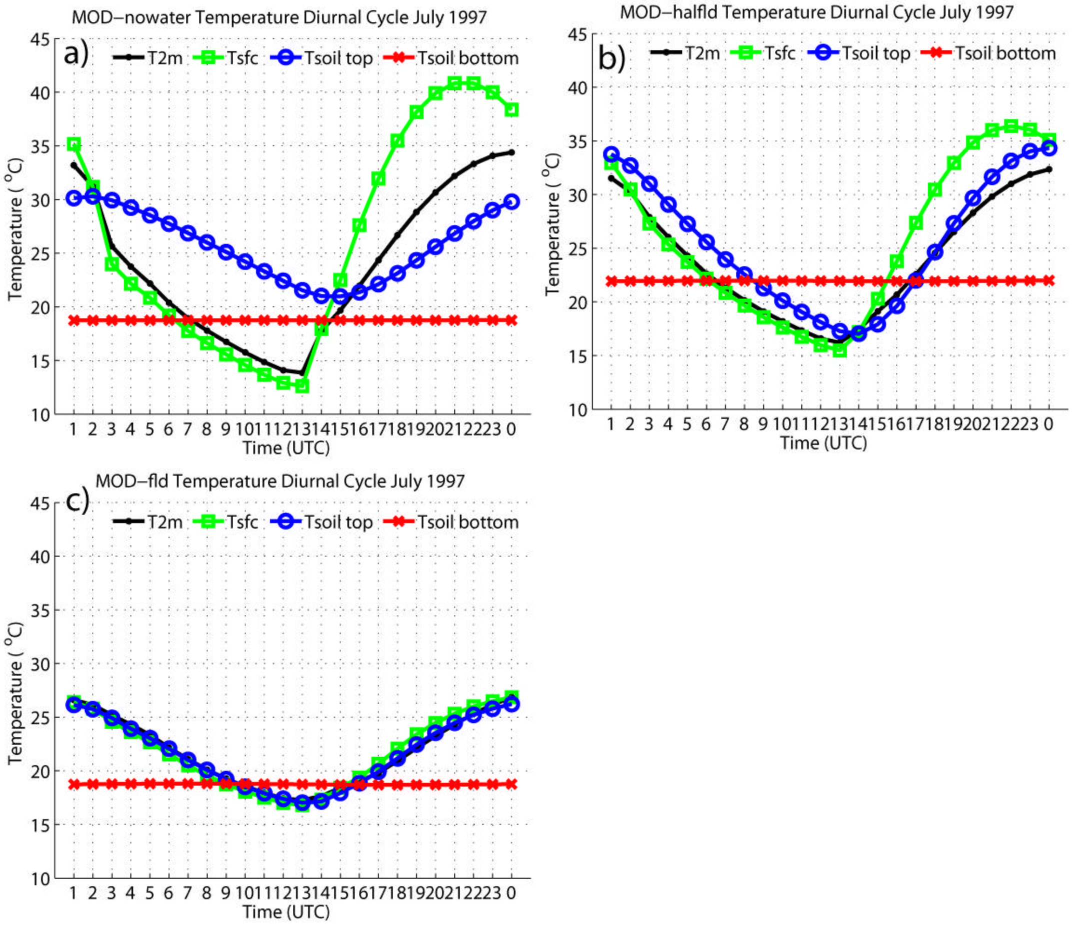

Figure 6 Diurnal cycle of near surface, surface skin, top soil layer, and bottom soil layer temperatures for July 1997. a) MOD-nowater, b) MOD-halfld, and c) MOD-fld.

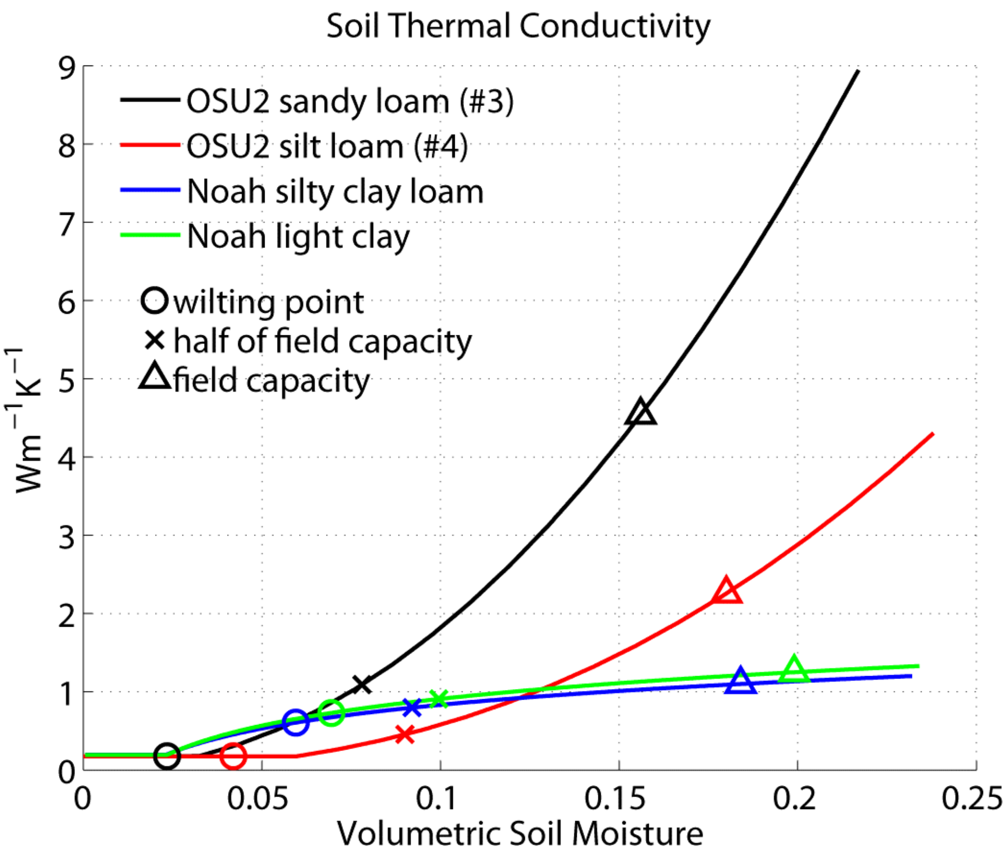

Figure 7 Soil thermal conductivity as a function of volumetric soil moisture for two soil types in RSM-OSU and two soil types in RSM-Noah.